LIMNOLOGY
and
OCEANOGRAPHY: METHODS

ASLO

Limnol. Oceanogr.: Methods 2020

doi: 10.1002/lom3.10371

Optimization of a subcellular metal fractionation method for fish liver: Homogenization, subcellular separation, and trial isolation of nuclear materials

Nastassia Urien,*[a] **Antoine Caron, Marc Lerquet, Patrice Couture, Peter G.C. Campbell**
Institut National de la Recherche Scientifique, Centre Eau Terre Environnement (INRS-ETE), Québec, Québec, Canada

Abstract

The subcellular compartmentalization of metals within aquatic organisms reflects their internal behavior after metal uptake and can provide important information about their potential toxicity. Commonly, the fractionation protocol used to determine subcellular metal partitioning in aquatic organisms consists of mechanically homogenizing the tissue, separating subcellular components into fractions by differential centrifugation and heat-denaturation steps, and determining the amount of metals associated with each fraction. However, the accurate separation of subcellular cell components is challenging and the nature and purity of the operationally defined subcellular fractions are rarely assessed. In the absence of this type of validation, however, the interpretation of subcellular metal fractionation results could be compromised. The aim of the present study was to adjust a subcellular fractionation protocol for the liver of field-collected fish and to test the adjusted protocol using fraction-specific enzyme markers. Overall, our results illustrate the need to optimize fractionation procedures when studying a new species or organ. In the course of this study, the categorization of some fractions was revised in accordance with the enzymatic results obtained, in order to yield a more credible subcellular fraction distribution scheme. In addition, trial assays aimed at isolating nuclear materials from the cellular debris were conducted, using DNA as a marker for nuclear material. Tested protocols failed to isolate the nuclei and results suggested that nuclei were probably trapped by disrupted cellular membranes. Recommendations on how to improve future subcellular fractionation studies on freshwater fish are discussed.

Investigations into the subcellular partitioning of metals within aquatic organisms are of major interest for ecotoxicological research. The results of such studies reflect how metals are handled within the cell (e.g., associated with sensitive target organelles or regulated/detoxified by binding to metallothioneins) and yield important information about potential metal toxicity or tolerance, and also are of possible relevance to metal trophic transfer (Wallace et al. 2003; Wallace and Luoma 2003). Typical subcellular partitioning protocols involve homogenization of the tissue of interest (disruption of cell membranes), the separation of the subcellular components into operationally defined fractions, and finally, the determination of the amount of metals associated with each fraction.

Homogenization is a crucial step because one must be careful to homogenize the sample strongly enough to ensure a high degree of breakage of cell membranes, but as gently as possible to avoid disrupting membrane-bound cellular organelles (e.g., mitochondria, lysosomes) which would cause leakage of their contents into other subcellular fractions (De Duve 1975; Graham 1997). Different approaches have been described in the literature to disrupt cell membranes (both mechanical and chemical; Klein et al. (1983); Simon et al. (2005); Lavoie et al. (2009)), nevertheless, for metal subcellular distribution studies, mechanical treatments are often favored as they avoid the addition of reagents that may introduce undesirable sources of metal contamination into samples and/or perturb metal speciation in the subcellular fractions (Rosabal et al. 2014; Cardon et al. 2018; Urien et al. 2018*a*).

After cell components are freed, their separation into subcellular fractions is usually achieved by successive differential centrifugation steps, a separation technique based on the settling velocities of the subcellular components, and heating steps (Kamunde and MacPhail 2008; Urien et al. 2018*a*). This

*Correspondence: nastassia.urien@edf.fr

[a]**Present address**: Electricité de France (EDF), Division Recherche et Développement (R&D), Laboratoire National d'Hydraulique et Environnement (LNHE), Chatou, France.

Additional Supporting Information may be found in the online version of this article.

is the most commonly used approach for metal partitioning studies, given its simplicity and minimal introduction of chemical reagents. However, using a differential centrifugation approach can be challenging as it can lead to various potential artifacts such as overlap among nominal subcellular fractions, since the size and density of the cell components may vary among organs and species (De Duve 1975).

Given the abovementioned artifacts that can be encountered during the fractionation protocol, existing subcellular fractionation procedures could clearly benefit from adjustments designed to maximize the separation of the subcellular fractions. Such adjustments would help improve the interpretation of the partitioning results (Cardon et al. 2018). However, in the literature, studies assessing the performance of fractionation protocols are surprisingly scarce. Among them, studies using enzymatic biomarkers specific to particular subcellular fractions (e.g., cytochrome *c* oxidase (CCO), specific to mitochondria; lactate dehydrogenase (LDH), a cytosolic enzyme) have yielded promising results (Hinton and Mullock 1997; Cardon et al. 2018; Khadra et al. 2019). In such studies, the activity of enzymatic markers is determined in each fraction in order to determine the relative contribution of each fraction to the total enzyme activity; the goal is to find the highest proportion of a marker in the subcellular fraction to which it is specific.

Fractionation protocols used in ecotoxicology studies typically yield up to six operationally defined subcellular fractions, considered either as sensitive to metals (mitochondria; lysosomes and microsomes; cytosolic enzymes) or detoxified (NaOH-resistant granules; cytosolic heat-stable proteins and peptides). The sixth fraction, often termed "cellular debris," contains cell membranes, unbroken cells and connective tissue, and nuclear materials. The presence of metals in this fraction is particularly difficult to interpret, notably because of its heterogeneous nature and our ignorance of the relative importance of the contributions of nuclei and debris to metal-binding in the fraction. A dominant association of the metals with the nuclei would clearly make this fraction fall into the metal-sensitive category. Given its ambiguous nature, most authors simply ignore this fraction (Cain et al. 2004) but there is a clear need to improve this branch of the fractionation protocol. To the best of our knowledge, no ecotoxicity studies have tackled this challenge to date.

In this context, the overall objective of the present study was to optimize the subcellular fractionation protocol for the liver of a freshwater fish species widespread in Canada, the white sucker (*Catostomus commersonii*), commonly used in biomonitoring studies. The specific objectives were: (1) to assess the efficiency of different homogenization methods; (2) to compare different subcellular separation protocols; and (3) to initiate trial assays to separate the nuclear materials from the cellular debris in the debris fraction. For objectives (1) and (2), LDH, citrate synthase (CS), CCO, and acid phosphatase (APHO) were used as specific enzymatic biomarkers of subcellular fractions. For objective (3), nuclei isolation involved filtration steps and separation efficiency was evaluated using DNA as a nuclear marker.

Materials and procedures

Collection and preservation of white sucker liver tissue

As described in one of our previous studies (Urien et al. 2018*b*), mature white suckers were caught in summer 2016 from two sites: a lake that was located downstream from a metal mining discharge and that exhibited a polymetallic contamination (As, Cd, Cu, Ni, Pb, Se, and Zn), and at a reference site (for details about the metal exposure gradient, *see* Urien et al. (2018*a*)). Briefly, upon capture (using gill nets), fish were immediately sacrificed by concussion and dissected to collect different organs, including the liver, and sex was determined. Organs were then placed in acid-washed 50-mL polypropylene tubes and put on dry ice until the return to the laboratory where they were immediately stored at −80°C until analysis. The capture and sampling protocols were approved by the INRS animal-care committee and the relevant governmental authorities issued scientific collector permits. For the purpose of the present study, only females from the reference lake were used (except for the "effect of tissue : buffer ratio" preliminary test where only females from the exposed lake were available). Fish of the same sex were chosen to avoid introducing confounding factors when interpreting enzymatic activity results.

Generic flowchart of the subcellular fractionation protocol

In the present study, various subcellular fractionation protocols were tested, with successive changes being based on the results of the previous modification. Thus, in this section, the generic fractionation protocol, based on the protocol used for white sucker by Urien et al. (2018*a*), is presented in order to help the reader to understand the procedures and to better identify the changes made to the different protocols tested (Fig. 1).

With respect to the homogenization step, frozen liver aliquots (≈ 0.5 g) were thawed on ice and ground in a Pyrex® Potter-Elvehjem tissue grinder with a motorized Teflon pestle in a cold isotonic buffer (Tris 25 mM, sucrose 250 mM) at a given tissue : buffer ratio (wet weight : volume of buffer). In the present study, the effects of changing the tissue : buffer ratio were examined and the efficiency of a two-step homogenization was tested.

After the homogenization, the sample ("homogenate", Fig. 1) was centrifuged at 1500 × *g* for 15 min at 4°C (centrifugation #1). The resulting supernatant (S1) was centrifuged at 15,000 × *g* for 45 min at 4°C (centrifugation #2) to collect the mitochondria (P2). The resulting supernatant (S2) was then centrifuged at 180,000 × *g* for 60 min at 4°C (centrifugation #3) to collect the lysosomes and microsomes in the pellet (P3), and the cytosol in the supernatant (S3). To assess cytosolic

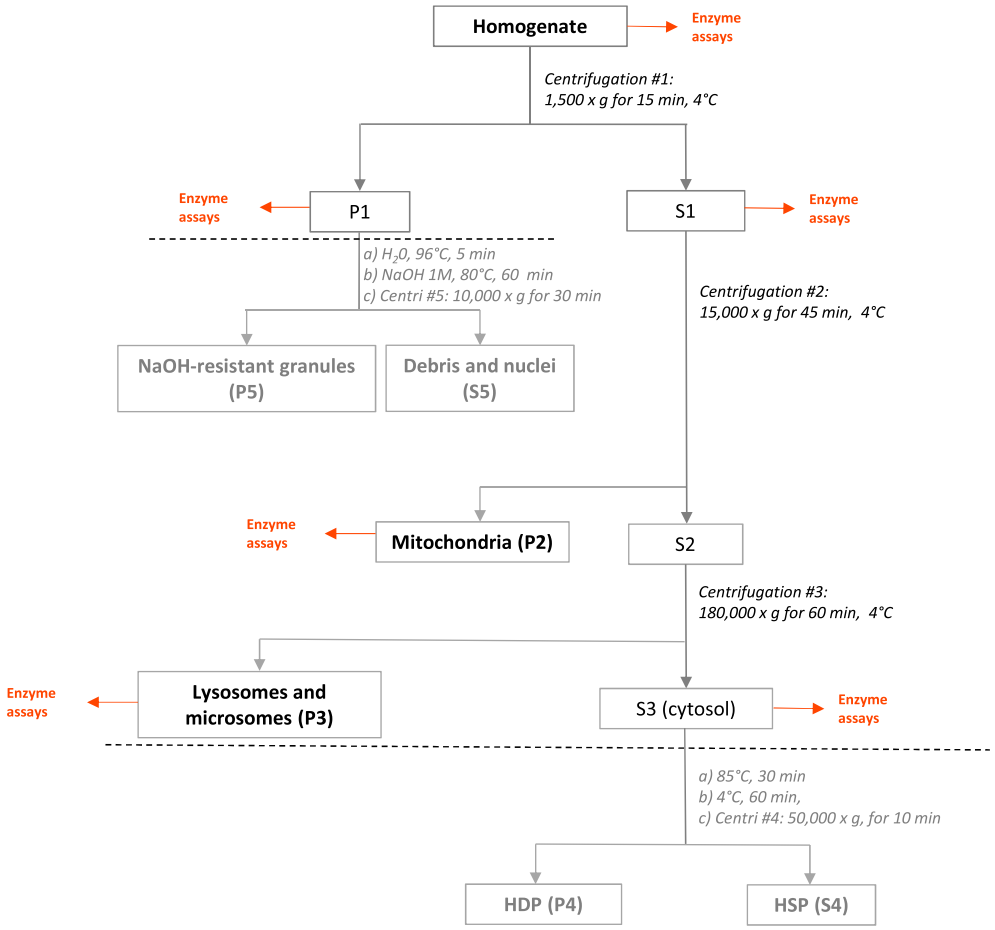

Fig. 1. Flowchart of the generic subcellular fractionation protocol for metal distribution studies. The letter P indicates pellet and S is for supernatant. The acronyms HSP and HDP mean, respectively, "heat-stable proteins" and "heat-denaturable proteins." The mention of "enzyme assays" indicates that marker enzymes can be measured in these fractions to validate the protocols. Fractions in gray and below the dotted lines were not subjected to enzyme assays as they had undergone heat treatments.

metal speciation, separation of the heat-denaturable proteins (HDP) and the heat-stable proteins (HSP) was performed by heating the cytosol at 85°C for 30 min. The cytosol was then cooled on ice for 60 min and centrifuged at $50{,}000 \times g$ for 10 min at 4°C (centrifugation #4). The heat-stable proteins (HSP) report to the supernatant (S4), whereas the pellet (P4) includes the heat-denaturable proteins (HDP).

The pellet from the original homogenization step (P1) was suspended in ultrapure water, heated at 96°C for 5 min and digested with NaOH (1 M) at 80°C for 60 min. The digestate was then centrifuged (#5) at $10{,}000 \times g$ for 30 min at room temperature (≈ 20°C) to recover the NaOH-resistant granules (P5). The supernatant (S5) contained the solubilized cellular debris and nuclear materials.

All centrifugation parameters were candidates for change during the protocol optimization.

In this study, centrifugations lower than $25{,}000 \times g$ were performed using an IEC Micromax microcentrifuge (Thermo Fisher Scientific). Centrifugations higher than $25{,}000 \times g$ were performed with a Sorvall™ WX Ultra 100 ultracentrifuge (Thermo Fisher Scientific) with a F50L-24x1.5 rotor (FIBERLite, Piramoon Technologies, USA) using 1.5 mL conical microtubes. All the protocols tested in the present study are detailed in Table 1.

Subcellular fractionation protocols tested

To refine the subcellular fractionation protocol, including evaluation of homogenization success, organelle integrity and subcellular fraction purity, we used enzyme markers specific to particular subcellular fractions: CCO, an enzyme specific to the mitochondrial membrane; CS, a mitochondrial biomarker located in the mitochondrial matrix; APHO, a lysosomal marker; and LDH, a cytosolic biomarker. For each tested condition, hepatic samples from two to three fish were tested. For each sample, enzyme reactions were performed in triplicate. The details of the enzyme analyses are described in the Supporting Information.

Table 1 Detailed descriptions of the subcellular fractionation protocols tested on white sucker livers for protocol optimization. Text in bold indicates a change compared to the previous tested protocol. The abbreviation "b.f.m." means back and forth movements.

#	*n*	Buffer ratio	Homogenization	Centrifugation type 1	Pellet resuspension + second homogenization	Centrifugation type 2	Pellet resuspension	Centrifugation type 3
I	3	1:3	• Potter-Elvehjem (570 rpm): 2 series of 5 b.f.m. with 30-s intervals on ice.	1500 × *g*, 15 min, 4°C	• 2× (150 μL buffer Tris-sucrose + 5 b.f.m. with a micropestle); • Centrifugation type 1	15,000 × *g*, 45 min, 4°C	• 200 μL buffer + 10 s vortex (8 W); • Centrifugation type 2	180,000 × *g*, 60 min, 4°C
II	2	1:3	• Potter-Elvehjem (570 rpm): **3 series** of 5 b.f.m. with 30-s intervals on ice.	1500 × *g*, 15 min, 4°C	• 2× (150 μL buffer Tris-sucrose + 5 b.f.m. with a micropestle); • Centrifugation type 1	**20,000** × *g*, 45 min, 4°C	• 200 μL buffer + 10 s vortex (8 W); • Centrifugation type 2	180,000 × *g*, 60 min, 4°C
III	2	1:3	• Potter-Elvehjem (570 rpm): 3 series of 5 b.f.m. with 30-s intervals on ice.	1500 × *g*, 15 min, 4°C	• **300 μL buffer Tris-sucrose ± 2 s vortex ± 5 sonication pulses (22 W, cycle 20%)**; • Centrifugation type 1	**25,000** × *g*, 45 min, 4°C	• **500 μL buffer** + 10 s vortex (8 W); • Centrifugation type 2	180,000 × *g*, 60 min, 4°C

Pool mitochondria and lysosomes + microsomes fractions → organelle fraction

#	*n*	Buffer ratio	Homogenization	Centrifugation type 1	Pellet resuspension + second homogenization	Centrifugation type 3	Pellet resuspension
IV	3	1:3	• Potter-Elvehjem (570 rpm): 3 series of 5 b.f.m. with 30-s intervals on ice.	1500 × *g*, 15 min, 4°C	• 300 μL buffer Tris-sucrose + **10 sonication pulses** (22 W, cycle 20%); • Centrifugation 1	180,000 × *g*, 60 min, 4°C	• No resuspension for this protocol
V	3	1:3	• Potter-Elvehjem (570 rpm): 3 series of 5 b.f.m. with 30-s intervals on ice.	1500 × *g*, 15 min, 4°C	• 300 μL buffer Tris-sucrose + 10 sonication pulses (**22–30 W**, cycle 20%); • Centrifugation 1	180,000 × *g*, 60 min, 4°C	• **300 μL buffer ± 10 s vortex (8 W);** • **Centrifugation type 3**

Note that fractions subjected to heat-treatment (HDP, HSP, debris+nuclei, and NaOH-resistant granules; in gray in Fig. 1) were not subjected to enzyme assays since heat-treatment and NaOH-digestion denature enzymes.

Effect of tissue : buffer ratio

Before starting the complete subcellular fractionation protocol, we performed preliminary assays to adjust the wet tissue weight : buffer volume ratio to be used for the homogenization. We hypothesized that the ratio might influence cell breakage efficiency since some tests did show that the suction force created in the tissue grinder (between the pestle and the glass) was more pronounced in more dilute solutions. Therefore, cell disruption efficiency was tested for ratios (A) 1 : 3 and (B) 1 : 8, using LDH assays on the livers of two exposed females (≈ 0.5 g of wet tissue, $n = 2$).

For these tests, limited protocols were applied, i.e., after homogenization only centrifugation #1 ($1500 \times g$ for 15 min at 4°C, Fig. 1) was performed to separate the pellet containing cellular debris from the supernatant containing the cytosol and the organelles (P1 and S1, respectively, in Fig. 1). LDH activity was then measured in these two fractions and in the homogenate. For tests A and B, the same homogenization protocol was used and consisted of three series of three back and forth movements with a glass Potter-Elvehjem tissue grinder (8 mL capacity in our case) equipped with a motorized Teflon pestle (570 rpm), with 30 s intervals on ice.

Effect of a two-step homogenization protocol

The efficiency of a two-step homogenization procedure was tested on two reference female liver samples ($n = 2$). First, a single-step homogenization was tested with two series of three (2×3) back and forth movements with the glass Potter-Elvehjem tissue grinder, with 30 s intervals on ice. The homogenate was centrifuged (centrifugation #1) to collect the pellet and supernatant. Second, a two-step homogenization was performed by applying the previous single-step homogenization and centrifugation, followed by resuspension of the resulting pellet with 300 μL of Tris-sucrose buffer and an additional homogenization step with 2×3 back and forth movements with the Teflon micropestle mounted on a stainless steel shaft driven by a cordless motor mixer (for use with 2.0 mL-capacity microtubes). The new homogenate was centrifuged again (#1) and the resulting supernatant was added to the previous supernatant obtained from the first centrifugation. LDH activity was measured in the supernatant (cytosol and organelles), the pellet (debris) and the homogenate. For these tests, about 0.5 g of wet tissue was used, and the tissue : buffer ratio was of 1 : 6.

Complete subcellular fractionation protocols.

It has been recently observed in the literature that a subcellular protocol that works for on species or organ does not necessarily fit for another (Rosabal et al. 2014; Cardon et al. 2018; Urien et al. 2018*a*; Khadra et al. 2019). Consequently, in the present study we chose to test different tools (Potter-Elvehjem tissue grinder, cordless motor mixer, sonication, etc.) in a "trial and error" mode, in order to best refine final subcellular fractionation protocol.

Once the tissue : buffer ratio had been chosen, five different subcellular fractionation protocols were successively tested (Table 1). To assess the influence of the modifications to the subcellular fractionation protocol and to compare results, the tested subcellular fractionation protocols and associated assays were performed on the liver of the same three individuals ($n = 3$, reference females). To avoid cycles of thawing/freezing each test day, several aliquots of liver tissue (≈ 0.5 g) were precut and preserved in microtubes at −80°C. Note that for the last test (#V), only ≈ 0.3 g of tissue was left but this portion was still used because it was important to keep the same individuals for robust comparison. This difference in mass is not expected to produce any effect on the results as the same tissue: buffer ratio was applied. However, to verify this assumption, we tested the effect of using different masses in the homogenization step and no difference was observed (the protocol and results are presented in the Supporting Information).

Quality control

As a quality control procedure, after each subcellular fractionation test, we carried out a test for loss of biological material during the partitioning of the homogenate. The original homogenate suspension was weighed accurately (Sartorius rc210 analytical scale ±0.01 mg), as was each of the fractions that were produced during the fractionation protocol. Additional buffer introduced for resuspension, if any, was considered. Average mass recovery, comparing the sum of the mass of each fraction with the original homogenate, fell in the 96–99% range.

To assess the quality of the enzyme activity measurements, activity recovery calculation was carried out by comparing total enzyme activity, estimated from aliquots of the whole tissue homogenate, with the sum of enzyme activities measured in the various subcellular fractions, as follows: [sum of enzyme activity in all the fractions/enzyme activity in the whole liver homogenate aliquot] × 100 (Cardon et al. 2018; Khadra et al. 2019): a percentage recovery between 70% and 130% was considered to be acceptable.

In order to extract the total enzyme activity from the fractions and homogenates, before measurements, samples were treated with a Triton X-100 buffer (1%; Molecular Grade, Fisher Scientific, in Tris buffer [25 mM, pH = 7.4]) and then mixed for 5 s with a vortex mixer (power = 10 W) and subjected to sonication (30 s pulse; duty cycle = 20%, power = 22 W, on ice). This step was sufficient to treat and resuspend pellet fractions for further enzymatic activity measurements (details of the enzyme analyses are given in the SI).

Attempted separation of nuclei from cellular debris

In the present study, we explored an approach based on the protocol proposed by Rickwood et al. (1997) to isolate

possible nuclear materials, with modifications. This approach relies on the use of differential centrifugation and filtration steps. First, ≈ 0.025 g of liver tissue was homogenized using the Teflon micropestle mounted on a stainless steel shaft driven by a cordless motor mixer for 3 s, five times, with 10-s intervals, in the homogenization buffer (Tris 25 mM, sucrose 250 mM, at a tissue : buffer ratio of 1 : 10). The resulting homogenate was centrifuged at $1200 \times g$ (and at $1500 \times g$ for the last test) for 10 min to separate the cytosol and organelles (supernatant) from the pellet that we considered to consist mainly of cellular debris, granules and nuclear materials. The pellet was then resuspended in 600 μL of Tris-sucrose buffer and filtered using a syringe filter to retain the debris and let nuclear materials go through (filtrate). Two types of filters were tested: a fiberglass mat of indeterminate porosity (not known but used as proposed in Rickwood et al. (1997)) and a nylon net filter with a nominal mesh size of 11 μm (nuclear material size expected to be around 5–7 μm diameter [Alberts et al. 2002]). The resulting filtrate was directly centrifuged at $1200 \times g$ (and at $1500 \times g$ for the last test) for 10 min in order to pellet the nuclei and any remaining debris. Finally, the resulting pellet was resuspended in 200 μL of dense sucrose buffer (2.2 M) and centrifuged at $70{,}000 \times g$ for 80 min to separate the nuclei (pellet) from remaining cellular debris (supernatant).

DNA was used as a marker for nuclei to evaluate the efficiency of the tested protocols. The DNA was extracted and measured using the *DNeasy® Blood & Tissue* kit (QIAGEN, Germany), following the instructions given by the manufacturer for DNA purification with a DNeasy Mini spin column. Briefly, samples were lysed by heat-treatment at 56°C for a minimum of 4 h with the detergent buffer provided with the kit in order to free the DNA. The resulting lysate was then loaded onto the spin column for purification and centrifuged to selectively bind the DNA to the column and let the rest of the sample pass through. The spin column containing the DNA was then washed to improve the purification and DNA was eluted with buffer (10 mM Tris-Cl, 0.5 mM EDTA, pH 9.0, to guarantee optimal recovery and stability of eluted DNA) for quantification by measuring the absorbance at 260 nm (Cary Bio 300 UV–visible spectrophotometer, Agilent). To increase DNA purity and avoid interference with RNA, RNAse A was added to the sample as instructed in the protocol, i.e., directly after the incubation at 56°C. DNA purity of the samples was checked by calculating a purity index as follows:

$$\frac{A_{260} - Bg_{320}}{A_{280} - Bg_{320}}$$

where A_{260} is the absorbance for DNA, A_{280} is the absorbance for RNA and Bg_{320} is the background absorbance for proteins. An index ranging from 1.7 to 1.9 indicates that the sample DNA purity is satisfactory. It is considered that one absorbance unit (U) at 260 nm is equivalent to 50 μg DNA/mL.

In the present study, DNA was first measured in an aliquot of the homogenate in order to estimate the total amount of DNA found in the homogenate aliquot that underwent the nuclei separation protocol described above. DNA was also measured in the resulting pellet (P1) that theoretically contained nuclear material as well as in the different supernatants resulting from the protocol, in order to express the quantity of DNA in a fraction as a percentage (%) of the total DNA in the homogenate. Unfortunately, it was not possible to measure the amount of DNA retained on the filter used to separate nuclei from cellular debris, as it proved to be extremely difficult to extract the residue on the filter once it had interacted with the latter. To circumvent this difficulty and estimate nuclear material loss during filtration, the separation protocol was performed with and without the filtration step and compared.

Three protocols were tested: (1) the protocol described above without the filtration step, (2) the protocol described above with a filtration step using the fiberglass mat described above (a 1.5-mL syringe filled with glass fiber to the 0.25 mL graduation), and (3) the protocol described above with a filtration step using the nylon net filter (11 μm) and a Swinnex Filter Holder system (EMD Millipore, Merck, Germany) and a centrifugation force of $1500 \times g$ instead of $1200 \times g$ (used in tests 1 and 2). To compare among the tests, the protocols were applied to the same three liver tissues of white sucker (n = 3).

Statistical analyses

Data for the tissue : buffer ratio and two-step homogenization tests are presented individually as two liver samples were used (no statistics). For the other tests, data are expressed as mean ± standard deviation (n = 3). For comparisons of percentage data, we applied arcsine transformation and nonparametric tests (Kruskal Wallis with a pairwise comparison post hoc test) were used as normal distribution and homoscedasticity could not be tested because of the low number of replicates.

Results

Effects of the buffer ratio on cell disruption

In this test, we used two tissue : buffer ratios (1 : 3, A; 1 : 8, B) and compared the cell membrane disruption efficacy by monitoring the relative proportions of LDH activity, a cytosolic enzyme, in the supernatant containing cytosol and the pellet with the cellular debris and unbroken cells. A high proportion of LDH in the pellet would indicate a high degree of unbroken cells, thus a low homogenization efficiency, whereas high proportions of LDH in the supernatant would indicate a better homogenization efficiency. Results are presented per individual in Fig. 2 (Ind. 1 and Ind. 2). They showed that, although interindividual variability was noteworthy, for a given individual, no changes between treatments A and B were detected, with proportions of LDH in the supernatant

equal to 65% and 69%, and to 85% and 86%, for individuals 1 and 2, respectively. These results indicate that changing the tissue : buffer ratios within the range that we tested had no influence on the homogenization efficiency of white sucker liver tissue.

For the subsequent experiments, the buffer ratio of 1 : 3 was selected as it enabled us to reduce reagent consumption and to limit tissue grinder volume (high volumes are likely to add practical difficulties in terms of container availability and compatibility with the centrifuge).

Effects of a two-step homogenization protocol

Two homogenization methods were tested and compared, the first using a single-step homogenization and the second introducing an additional step of resuspension and homogenization of the pellet resulting from the first centrifugation. To evaluate the effects on cell disruption, we measured LDH activity in the resulting final pellet (containing cellular debris and unbroken cells) and supernatant (containing the cytosol and organelles). The results, presented in Fig. 3, show that with the single-step homogenization protocol approximately half of the LDH activity was located in the supernatant (50% and 58%, respectively for individuals 1 and 2). The LDH proportions in the supernatant increased from 50% to 74% and 58% to 83%, for individuals 1 and 2, respectively, with the two-step homogenization protocol; this result clearly demonstrates that a two-step homogenization protocol improved cell disruption efficiency.

Evaluation of the complete subcellular fractionation protocols

In the following assessment, we measured and compared the enzyme activity results for LDH, CCO, CS, and APHO in each isolated fraction for all tested protocols. *In fine*, the goal was to select the protocol that allowed an optimal trade-off between an efficient cell disruption and clear fraction separation. The presented protocols (Table 1) were gradually adapted as a function of the results of the previous protocol tested. To assess our protocol efficiency, we selected several criteria. First, with respect to cell disruption during homogenization, we attempted to achieve maximum LDH activity in the cytosol fractions with a minimum in the debris fraction; minimum CCO and CS activity in the debris fraction was also desirable. Secondly, our goal for the fractionation of the subcellular components was to have the highest CCO and CS activity in the mitochondrial fraction (CCO, a mitochondrial membrane enzyme, as a marker of mitochondrial presence and CS, a matrix enzyme, as a marker of mitochondrial integrity), and the highest APHO activity in the lysosomes and microsomes fraction. The proportions of enzyme activities in each fraction are given in Fig. 4 for protocols # I to # V and are also available in detail in Table S1 of the Supporting Information.

Homogenization procedure

Based on the preceding results (Fig. 3), we adopted the two-step homogenization method for all tested protocols (# I to V); the parameters chosen for the homogenization step varied according to the protocol (*see* Table 1). With respect to cell breakage efficiency, the procedure combining the use of the Potter-Elvehjem tissue grinder equipped with a motorized Teflon pestle and sonication (# III to V) yielded better results than the protocols # I to II where sonication was not used. Indeed, comparison of the proportions of LDH, CCO and CS activities in the debris fraction for protocols # I and # V showed a dramatic decrease of activity, from 34% ± 8% to 10% ± 2% for LDH, from 38% to 6% ± 1% for CCO and from 15% ± 1% to 4% ± 1% for CS (Fig. 4 and Table S1). Results also suggest that with protocols # III to V, only a small proportion of white sucker liver cells remained intact following homogenization. However, regardless of the protocol, the proportions of the LDH activity in the cytosolic fraction remained

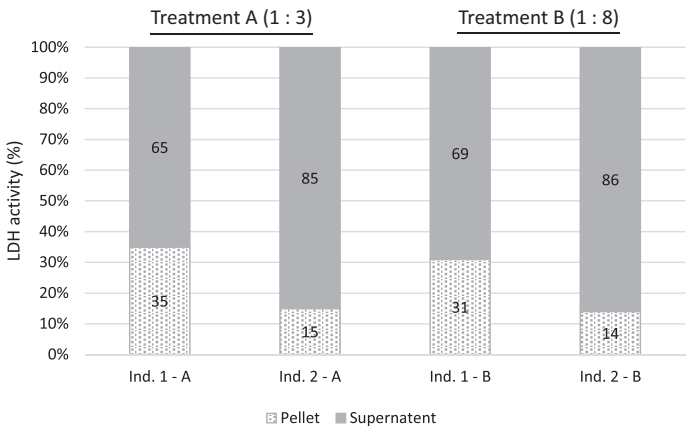

Fig. 2. Distribution of LDH enzymatic activities (in percentage of the total activity) between the cellular debris fraction (pellet) and the cytosol (supernatant) of white sucker liver, for two individual fish.

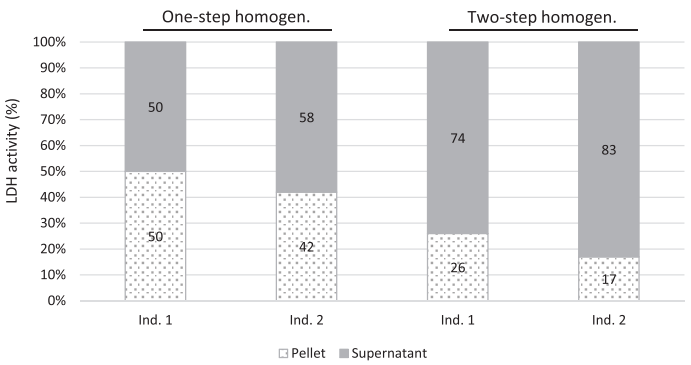

Fig. 3. Proportions of LDH enzyme activities (in percentage of the total activity) in the cellular debris fraction (pellet) and the cytosol (supernatant) of two white sucker liver samples, without ("one-step homogenization") and with the additional resuspension/homogenization step ("two-step homogenization").

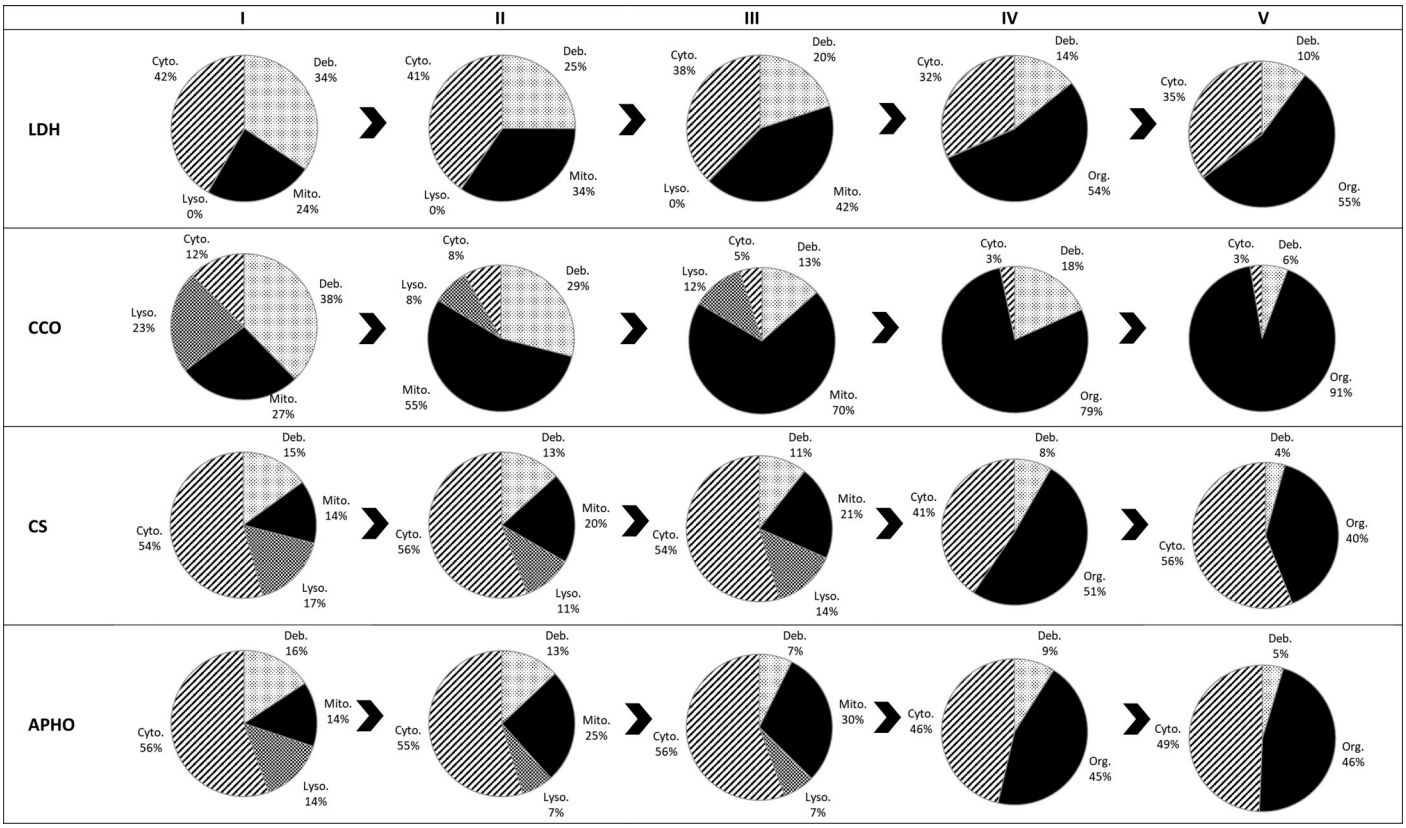

Fig. 4. Mean proportion of enzymatic activities (in percentage, n = 3) recovered in each fraction for each subcellular fractionation protocol tested for white sucker liver (protocols #I to V, n = 3, except for CCO activity for treatments I and III, n = 2. For more details, *see* Table S1 in the Supporting Information). Deb., debris and nuclei; Mito., mitochondria; Lyso., lysosomes and microsomes; Cyto., cytosol; org., organelles. Pie slice legend: Black = mitochondria for protocols # I to # III and organelles for protocols # IV to # V; hatching = cytosol; dense stippling = lysosomes and microsomes; light stippling = debris and nuclei.

quite low, ranging from 32% to 42%. In comparison, in rainbow trout, Cardon et al. (2018) achieved proportions of the LDH activity in the cytosol greater than 70%. The rest of the LDH activity was found in the fraction containing mitochondria (Fig. 4), suggesting that some of the cytosol may have been trapped in this fraction (this observation is further addressed later). Finally, the best protocol regarding cell disruption was # V, combining three series of five back and forth movements with a Potter-Elvehjem tissue grinder equipped with the motorized Teflon pestle and 10 sonication pulses. Note that the duration and intensity of the sonication should be carefully controlled, as this step may cause damage to the samples through inadvertent heating, leading to enzyme denaturation that would affect enzyme activity measurements.

Fraction separation

During preliminary assays, we noticed the formation of variable amounts of a whitish intermediate layer between the mitochondrial pellet and the supernatant after centrifugation #2 (Fig. 1). This layer, likely of lipidic nature, was also observed and characterized by Cardon et al. (2018) in their study of rainbow trout; they reported that this layer contained a mix of mitochondrial matrix and cytosol. In our case, this layer was not fully homogenous and seemed to contain cytosol pockets. To yield a better mitochondrial fraction, we decided to apply a two-step mitochondrial pelleting for each tested protocol. After centrifugation #2 (Fig. 1 and Table 1), the mitochondrial pellet obtained, with the intermediate layer on top (we assumed that it was better to collect less supernatant to avoid contaminating it with the intermediate layer), was resuspended with the Tris-sucrose buffer, mixed with a vortex mixer and then subjected to a second centrifugation #2 (Table 1). In this manner, the mitochondrial pellet was cleanly separated and collection of the supernatant was facilitated.

With respect to the operationally defined mitochondrial fraction, the increase of the centrifugal force for centrifugation #2 (protocols # I to III; 15,000 × g ⊠ 25,000 × g, Table 1) led to improved mitochondrial pelleting with, for CCO, an increase of its partitioning into the mitochondrial fraction (27–70%, Fig. 4 and Table S1). A reasonable proportion of CCO activity was present in the lysosome and cytosol fractions. However, regardless of the protocol, roughly half of the CS activity systematically reported to the cytosol fraction, indicating that mitochondrial integrity had been compromised. Even with

Table 2 Estimated amount of DNA in the homogenate used for tests (1) to (3) (in μg of DNA), sum of DNA measured in each fraction after applying the procedures for tests (1) to (3) (μg of DNA), percentage loss of DNA during the procedures (in %), and proportion of DNA found in the putative nuclei fraction with respect to the sum of DNA in each fraction (in %).

		Estimated total DNA (μg)	Σ DNA in each fraction (μg)	% loss of DNA	% DNA in "nuclei" related to the sum of DNA in each fraction
Test (1)—without filtration	Ind. 1	58.3	20.8	64.3%	92%
	Ind. 2	41.0	22.9	44.1%	84%
	Ind. 3	35.5	23.9	32.8%	90%
Mean				47%	88%
SD				16%	4%
Test (2)—with filtration (fiberglass)	Ind. 1	51.7	5.0	90.3%	62%
	Ind. 2	94.6	3.8	96.0%	28%
	Ind. 3	46.0	3.6	92.2%	27%
Mean				93%	39%
SD				3%	20%
Test (3)—with filtration (nylon net)	Ind. 1	139.4	9.57	93.1%	37%
	Ind. 2	77.4	5.49	92.9%	22%
	Ind. 3	91.7	NA		
Mean				93%	30%
SD				0%	11%

protocol # I, which had the gentlest homogenization method, 54% ± 8% of the CS activity was found in the cytosol fraction (Fig. 4 and Table S1). Similarly, almost 50% of APHO activity was concentrated in the cytosol, regardless of the protocol applied, indicating that lysosomes were also damaged even with the gentlest homogenization procedure.

These results raised questions about the significance and credibility of the lysosomes and microsomes fraction. Therefore, in protocols # IV and V, we combined the "lysosomes and microsomes" and "mitochondria" fractions by directly applying ultracentrifugation (centrifugation #3 in Fig. 1) to the supernatant S1 resulting from centrifugation #1. The combined fraction was designated as "organelles." In addition, this choice was reinforced by the fact that in our previous study (Urien et al. 2018*a*), the contribution from the lysosome and microsome fraction to the total metal(loid) burden was negligible compared to that observed in the mitochondria. In principle, this combination should not affect the interpretation of the subcellular metal partitioning data.

The proportion of CCO activity in the organelle fraction was higher than that obtained with protocols # I to III in the fraction "mitochondria" (Fig. 4 and Table S1). By including organelle pellet resuspension (in protocol # V), the CCO activity proportion reached 91% ± 1% in the organelle fraction. Concerning CS activity, the proportion found in the organelles was greater than the proportion found in the previous "mitochondria" fraction (up to 50% with protocol # IV compared to a maximum of 21% with protocol # III, Fig. 4 and Table S1). Nevertheless, half of the CS activity was still found in the cytosol, indicating the leakage of mitochondrial content. The activity of the lysosomal marker, APHO, was equally distributed between the cytosol and the organelles.

Trial isolation of the nuclei from the debris fraction

In the present study, we tried to separate nuclear materials from the debris with a protocol based on filtration and centrifugation steps and we used DNA as the nuclei marker. The proportions of DNA found in the isolated nuclei and the percentage loss of DNA during the procedure are presented in Table 2. Results showed that the protocol applied without the filtration step (test (1)) resulted in an average DNA loss of 47% ± 16%, which suggests that roughly half of the nuclear material was lost during the procedure, likely because of adsorptive losses to the tube walls during successive tube changes. Note, however, that with test 1, the major part of remaining DNA was found in the nuclei + debris fraction (88% ± 4% of the DNA that had not been lost to this assumed adsorption).

In comparison, the addition of a filtration step (with the fiberglass mat, test (2); with a nylon net, test (3)) showed a constant and much greater loss of DNA, 93% loss in both cases. Given the difference in DNA recovery between test (1) on one hand and tests (2) and (3) on the other hand, these results suggest that DNA was probably retained on the filter (nevertheless, it was not possible to extract DNA from the filter to measure it). Finally, DNA found in the nuclei + debris fraction after tests (2) and (3) was very low (between 39% and 30% when compared to the sum of DNA found in each fraction and less than 5% when considering estimated total DNA from the original homogenate). The relative comparison of

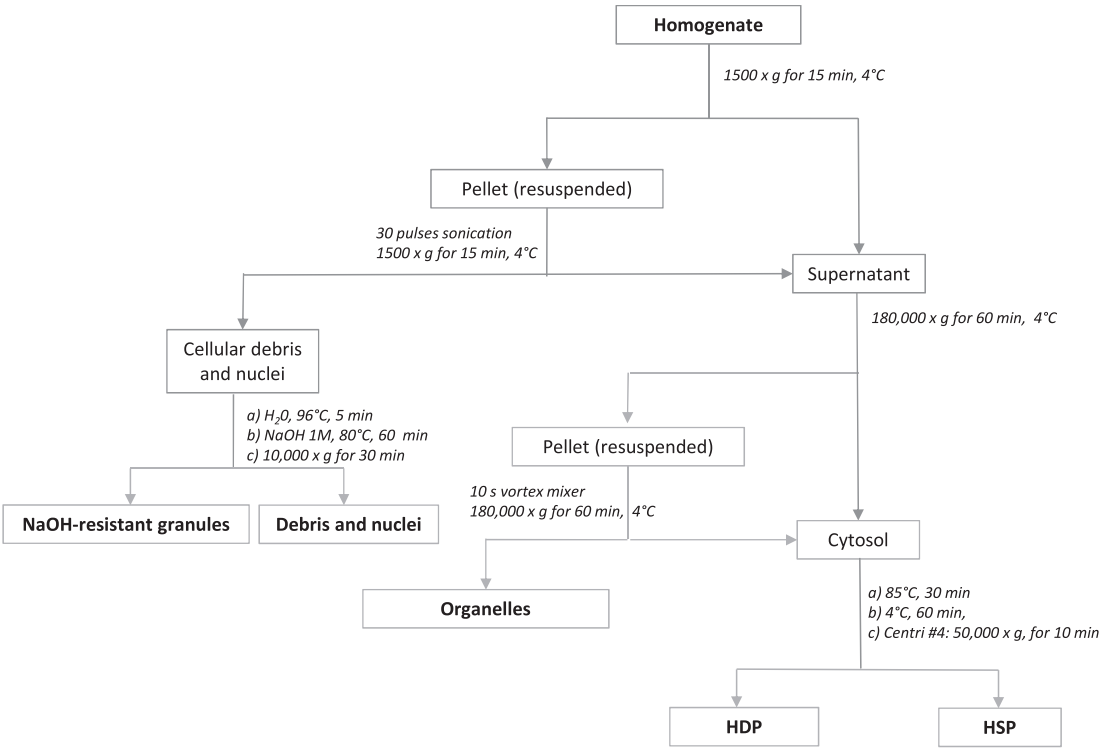

Fig. 5. Flowchart of the most promising subcellular fractionation protocol (# V) for white sucker livers. HSP for heat-stable proteins; HDP for heat-denaturable proteins.

the three protocols (Table 2) showed that even if the porosity of the filter was theoretically large enough to allow nuclei to pass through, most of the nuclear material was retained by the filter. These results suggest that filtration is not appropriate for the isolation of nuclear material from cells in this context.

Discussion

The aim of the present study was to optimize a subcellular fractionation protocol for the liver of white suckers and in this manner improve the interpretation of such partitioning results in future studies of white sucker. Our results clearly demonstrate that optimization of such protocols is a necessary step. In the following sections, we discuss the implications of the homogenization and fraction separation results, which impinge on how subcellular metal partitioning results can be interpreted. Finally, based on this work, some recommendations are proposed to guide readers who are planning to study subcellular metal partitioning in biota.

Homogenization step

Tissue homogenization is a critical step during the subcellular fractionation process, because one must maximize cell disruption to ensure that subsequent subcellular fractionation will be representative for the whole cell tissue, while limiting damage to the organelles. For white sucker, a two-step homogenization, using a glass Potter-Elvehjem tissue grinder with additional sonication was the best option to achieve efficient cell breakage. These results agree with other studies that have reported that performing a double-step homogenization improved cell disruption efficiency; examples of the types of tissue that were homogenized include the liver and the gonads for *Perca flavescens* and the liver for *Oncorhynchus mykiss*, as well as whole organisms for *Daphnia magna* and *Chaoborus* sp. (Cardon et al. 2018; Khadra et al. 2019). In addition, concerning rainbow trout, Cardon et al. (2018) recommended use of sonication for the second step homogenization, as in our fish study.

The relative contribution from the debris fraction to the total metal burden can be used as an indicator of homogenization efficiency: a low and constant percentage contribution indicates that the homogenization step is both effective and reproducible (Rosabal et al. 2014). The presence of a high proportion of unbroken cells in the debris fraction can bias or hinder the interpretation of subcellular metal partitioning results, since subsequent fractionation will not be representative of the whole tissue sample that was subjected to homogenization. The corollary is that it is advisable to adjust the homogenization step for each organ and even for each species. In the present study, and according to the LDH activity in the debris fraction, protocol # V enabled us to achieve ≈ 90% cell disruption (LDH in debris = 10%), which can be considered as satisfactory.

Regardless of the homogenization protocol used (# I to V), half (50%) of the mitochondrial and lysosomal content was detected in the cytosol (*see* CS and APHO in cytosol, Fig. 4). These results indicate that these organelles were damaged, but as the apparent degree of damage remained approximately constant for all protocols, even for protocol # I, considered to be the gentlest, it is difficult to attribute this damage to the homogenization method used. After their collection, fish tissues were stored at −80°C. In a recent study, Cardon et al. (2018) reported that using fresh samples of *Chironomus* and rainbow trout decreased mitochondria leakage compared to frozen samples (e.g., 70% of CS activity was found in the cytosol in frozen *Chironomus* vs. 25% in fresh insects). Therefore, in our study, it is reasonable to think that storage at −80°C could have led to weakening of organelle membranes (mitochondria and lysosomes at least). Nevertheless, studying field-collected aquatic organisms often involves a freezing step at −80°C or −196°C for conservation, a step that is rarely avoidable. Thus, before applying a subcellular fractionation protocol to frozen samples, it is clearly advisable to assess the protocol as we have done in the present study, to avoid misinterpretation of the subsequent subcellular metal partitioning data.

Fraction separation

It is usually accepted that after a centrifugation at ~ $15{,}000 \times g$, mitochondria will pellet and smaller organelles such as lysosomes and microsomes will remain in the supernatant and could be then pelleted by ultracentrifugation ($\geq 100{,}000 \times g$). In our study, a centrifugation force of $25{,}000 \times g$ was necessary to yield the best proportion of CCO activity (mitochondrial marker) in the operationally defined mitochondria fraction. Nevertheless, the mitochondria separation was hindered by the presence of an intermediate layer of variable importance located on top of the mitochondria pellet. Similar observations were reported by Cardon et al. (2018) for rainbow trout and by Urien et al. (2018*a*) for white sucker, but not for insects (Rosabal et al. 2014; Cardon et al. 2018). To circumvent this artifact, a resuspension of the mitochondrial pellet was necessary.

In the course of this study, the assessment of different subcellular fractionation protocols (# I to V) led us to rethink the operationally defined subcellular fractions that are usually collected in studies of subcellular metal partitioning in aquatic organisms. We combined some fractions to yield a subcellular fraction distribution scheme that better reflected the results obtained with the marker enzymes. This was the case for the "mitochondria" and the "lysosomes and microsomes" fractions. For example, APHO activity (lysosomal marker) in the operationally defined lysosomes and microsomes fraction accounted for a maximum of only 14% of the total activity, indicating that this fraction contained few intact lysosomes. In contrast, 30% of the APHO activity was found in the mitochondria fraction and about 50% in the cytosol, which led us to reconsider the lysosomal fraction (Fig. 4) and to collect instead a combined "organelles" fraction (mitochondria + lysosomes + microsomes). Some authors consider that a centrifugation force greater than $10{,}000 \times g$ collects not only mitochondria but also lysosomes in the pellet, for cuttlefish and bivalves (Simon et al. 2005; Bustamante et al. 2006). This overlap could explain the 30% APHO activity found in the mitochondria in protocol # III, where a centrifugation force of $25{,}000 \times g$ was used to pellet mitochondria. In a recent study of rainbow trout, Cardon et al. (2018) also suggested that lysosomes and mitochondria could be combined in the same fraction.

Regarding LDH activity (cytosol marker) in the cytosol, our results yielded proportions of about 35% on average, which is low with respect to the criterion of "minimum 70 % of LDH in the cytosol fraction of rainbow trout", as defined by Cardon et al. (2018). Despite resuspension of the pellet and recentrifugation, LDH activity remained important in the mitochondria and organelle fractions. One explanation could be that a slight amount of cytosol remained; however, trapped in the mitochondria or organelle fractions during the process, despite our efforts. On the other hand, a study by Brooks et al. (1999) suggested that LDH could be a constituent part of mitochondria in rat liver; our results suggest that this may also be the case in white sucker livers.

Finally, the protocol that achieved the best subcellular fractionation results in our study is summarized in Fig. 5. Note that the application of the complete protocol will depend on the number of samples to treat, but without considering homogenization time, the whole subcellular fractionation procedure will roughly take 6–7 h. It is also possible to reduce time by performing some steps in parallel.

Finally, compared to other studies in the literature, this work supports the fact that subcellular fractionation protocols should be species-specific. Note too that this protocol was adapted for fish collected in the same seasonal period, and we cannot exclude the possibility that variation in tissue composition (e.g., as a function of season, breeding status, nutritional level, etc.) might affect the efficiency of the subcellular fractionation protocol. In the literature, there are different studies dealing with subcellular fractionation, in particular in Yellow perch, caught in different lakes, at different times of the year and under different conditions, and none of them have identified such variations. (Campbell et al. 2005; Giguère et al. 2006). Nevertheless, the question deserves to be asked and further investigation into the possible influence of confounding factors likely to affect subcellular fractionation efficiency would be of great value for ecotoxicological studies.

Trial isolation of the nuclei

Knowledge of the relative proportions of metals bound to nuclear materials vs. cellular debris would greatly improve our interpretation of subcellular metal distribution data. Binding of nonessential metals to nuclear material might be expected to lead to deleterious effects (Pierron et al. 2011; Omar

et al. 2012; Palermo et al. 2015). However, separation of the nuclei from the debris fraction is challenging. The results of our trial separation of nuclear materials from the cellular debris indicated that none of the tested protocols were successful in concentrating the nuclear material; the relative contribution of the putative nuclei fraction to the total DNA, used as a nuclei marker, was very low. A possible explanation could be that the nuclei were retained within the cellular debris on the filter. We speculate that cell membranes, once disrupted, may close upon themselves as droplets and enclose nuclear materials. Nuclei might also be trapped within connective tissue, forming large agglomerates that were retained by the filters. This hypothesis has been discussed in the recent study of Cardon et al. (2018) and supported by scanning electron microscopy (*see* details in the SI of their article).

It is also important to note that the measurement of DNA is not specific and does not discriminate between nuclear DNA and mitochondrial DNA. As we previously showed in the section entitled Fraction separation, the mitochondrial matrix tended to leak during the fractionation procedure, and it is possible that nuclear DNA could have been contaminated with mitochondrial DNA during our trials. This hypothesis is reinforced by the presence of a low DNA signal in the supernatant following the first centrifugation, which should contain the cytosol and organelles including mitochondria and mitochondrial DNA. Further development is needed to achieve an effective isolation of nuclei, and markers other that DNA should be tested to detect nuclear materials and allow assessment of different nuclei isolation protocols.

Recommendations

The present study highlights the need to verify the efficiency of different fractionation protocols and illustrates the use of enzyme markers to validate protocols. In addition, the use of such enzyme markers is relatively easy and not too costly. In this last section, we put forward some recommendations regarding subcellular fractionation protocols to improve future studies on freshwater fish.

- The fraction content should be verified for each new species and organ for correct interpretation of subcellular metal partitioning. Some adaptation of the procedure may be necessary to avoid the collection of overtly ambiguous fractions.
- Particular attention should be paid to fraction integrity when working with frozen samples.
- A two-step homogenization procedure is strongly recommended to increase cell breakage efficiency.
- The resuspension and recentrifugation of the organelle pellet are recommended to improve fraction purity.
- In cases where an intermediate layer appears in the step designed to collect the organelles (including mitochondria), it is recommended that the pellet with the layer on the top be resuspended. If this is not possible, we recommend combining this layer with the pellet rather than the supernatant, to limit contamination of the cytosol.

References

Alberts, B., A. Johnson, J. Lewis, M. Raff, K. Roberts, and P. Walter. 2002. Molecular biology of the cell, 4th Edition. Garland Science Taylor & Francis Group.

Brooks, G. A., H. Dubouchaud, M. Brown, J. P. Sicurello, and C. E. Butz. 1999. Role of mitochondrial lactate dehydrogenase and lactate oxidation in the intracellular lactate shuttle. Proc. Natl. Acad. Sci. USA **96**: 1129–1134. doi:10.1073/pnas.96.3.1129

Bustamante, P., M. Bertrand, E. Boucaud-Camou, and P. Miramand. 2006. Subcellular distribution of Ag, Cd, Co, Cu, Fe, Mn, Pb, and Zn in the digestive gland of the common cuttlefish *Sepia officinalis*. J. Shellfish. Res. **25**: 987–994. doi:10.2983/0730-8000(2006)25[987:SDOACC]2.0.CO;2

Cain, D. J., S. N. Luoma, and W. G. Wallace. 2004. Linking metal bioaccumulation of aquatic insects to their distribution patterns in a mining-impacted river. Environ. Toxicol. Chem. **23**: 1463–1473. doi:10.1897/03-291

Campbell, P. G. C., A. Giguère, E. Bonneris, and L. Hare. 2005. Cadmium-handling strategies in two chronically exposed indigenous freshwater organisms—the yellow perch (*Perca flavescens*) and the floater mollusc (*Pyganodon grandis*). Aquat. Toxicol. **72**: 83–97. http://dx.doi.org/10.1016/j.aquatox.2004.11.0

Cardon, P.-Y., A. Caron, M. Rosabal, C. Fortin, and M. Amyot. 2018. Enzymatic validation of species-specific protocols for metal subcellular fractionation in freshwater animals. Limnol. Oceanogr.: Methods **16**: 537–555. doi:10.1002/lom3.10265

De Duve, C. 1975. Exploring cells with a centrifuge. Science **189**: 186–194. http://dx.doi.org/10.1126/science.1138375

Giguère, A., P. G. C. Campbell, L. Hare, and P. Couture. 2006. Sub-cellular partitioning of cadmium, copper, nickel and zinc in indigenous yellow perch (*Perca flavescens*) sampled along a polymetallic gradient. Aquat. Toxicol. **77**: 178–189. http://dx.doi.org/10.1016/j.aquatox.2005.12.001

Graham, J. M. 1997. Homogenization of tissues and cells, p. 1–29. *In* J. M. Graham, D. Rickwood, and B. D. Hames [eds.], Subcellular fractionation—a practical approach. Oxford Univ. Press.

Hinton, R. H., and B. M. Mullock. 1997. Isolation of subcellular fractions, p. 31–69. *In* J. M. Graham, D. Rickwood, and B. D. Hames [eds.], Subcellular fractionation—a practical approach. Oxford Univ. Press.

Kamunde, C., and R. MacPhail. 2008. Bioaccumulation and hepatic speciation of copper in rainbow trout (*Oncorhynchus mykiss*) during chronic waterborne copper exposure. Arch. Environ. Contam. Toxicol. **54**: 493–503. doi:10.1007/s00244-007-9046-9

Khadra, M., A. Caron, D. Planas, D. E. Ponton, M. Rosabal, and M. Amyot. 2019. The fish or the egg: Maternal transfer and subcellular partitioning of mercury and selenium in yellow perch (*Perca flavescens*). Sci. Total Environ. **675**: 604–614. doi:10.1016/j.scitotenv.2019.04.226

Klein, U., C. Chen, M. Gibbs, and K. A. Platt-Aloia. 1983. Cellular fractionation of *Chlamydomonas reinhardii* with emphasis on the isolation of the chloroplast. Plant Physiol. **72**: 481–487. doi:10.1104/pp.72.2.481

Lavoie, M., J. Bernier, C. Fortin, and P. G. Campbell. 2009. Cell homogenization and subcellular fractionation in two phytoplanktonic algae: Implications for the assessment of metal subcellular distributions. Limnol. Oceanogr.: Methods **7**: 277–286. doi:10.4319/lom.2009.7.277

Omar, W. A., K. H. Zaghloul, A. A. Abdel-Khalek, and S. Abo-Hegab. 2012. Genotoxic effects of metal pollution in two fish species, *Oreochromis niloticus* and *Mugil cephalus*, from highly degraded aquatic habitats. Mutat. Res. Toxicol. Environ. Mutagen. **746**: 7–14. doi:10.1016/j.mrgentox.2012.01.013

Palermo, F. F., W. E. Risso, J. D. Simonato, and C. B. R. Martinez. 2015. Bioaccumulation of nickel and its biochemical and genotoxic effects on juveniles of the neotropical fish *Prochilodus lineatus*. Ecotoxicol. Environ. Saf. **116**: 19–28. doi:10.1016/j.ecoenv.2015.02.032

Pierron, F., E. Normandeau, M. A. Defo, P. G. C. Campbell, L. Bernatchez, and P. Couture. 2011. Effects of chronic metal exposure on wild fish populations revealed by high-throughput cDNA sequencing. Ecotoxicology **20**: 1388–1399. doi:10.1007/s10646-011-0696-z

Rickwood, D., A. Messent, and D. Patel. 1997. Isolation and characterization of nuclei and nuclear subfractions, p. 71–105. *In* J. M. Graham, D. Rickwood, and B. D. Hames [eds.], Subcellular fractionation—a practical approach. Oxford Univ. Press.

Rosabal, M., L. Hare, and P. G. C. Campbell. 2014. Assessment of a subcellular metal partitioning protocol for aquatic invertebrates: Preservation, homogenization, and subcellular fractionation. Limnol. Oceanogr.: Methods **12**: 507–518. doi:10.4319/lom.2014.12.507

Simon, O., V. Camilleri, G. Grasset, and J. Garnier-Laplace. 2005. Subcellular fraction associated to radionuclide analysis in various tissues: Validation of the technique by using light and electron observations applied on bivalves and uranium. Radioprotection **40**: S199–S204. doi:10.1051/radiopro:2005s1-031

Urien, N., S. Cooper, A. Caron, H. Sonnenberg, L. Rozon-Ramilo, P. G. C. Campbell, and P. Couture. 2018a. Subcellular partitioning of metals and metalloids (As, Cd, Cu, Se and Zn) in liver and gonads of wild white suckers (*Catostomus commersonii*) collected downstream from a mining operation. Aquat. Toxicol. **202**: 105–116. doi:10.1016/j.aquatox.2018.07.001

Urien, N., S. Jacob, P. Couture, P. G. C. Campbell. 2018b. Cytosolic distribution of metals (Cd, Cu) and metalloids (As, Se) in livers and gonads of field-collected fish exposed to an environmental contamination gradient: An SEC-ICP-MS analysis. Environments **5**: 102. doi:10.3390/environments5090102

Wallace, W. G., and S. N. Luoma. 2003. Subcellular compartmentalization of Cd and Zn in two bivalves. II. Significance of trophically available metal (TAM). Mar. Ecol. Prog. Ser. **257**: 125–137. http://dx.doi.org/10.3354/meps257125

Wallace, W. G., B.-G. Lee, and S. N. Luoma. 2003. Subcellular compartmentalization of cd and Zn in two bivalves. I. Significance of metal-sensitive fractions (MSF) and biologically detoxified metal (BDM). Mar. Ecol. Prog. Ser. **249**: 183–197. doi:10.3354/meps249183

Acknowledgments

The authors would like to thank O. Gosselin, L. Rozon-Ramilo and H. Sonnenberg who participated in the fieldwork, and S. Cooper for her preliminary work on subcellular fractionation protocol optimization with white suckers. P.G.C.C. was supported by the Canada Research Chairs program. We also thank the industrial partner, Stantec Consulting Ltd., and the Natural Sciences and Engineering Research Council of Canada (NSERC) for cofunding this study.

Conflict of Interest

None declared.

Submitted 22 November 2019
Revised 25 March 2020
Accepted 03 May 2020

Associate editor: Clifton Buck